Preparation of the extruded UiO-66-based Metal-Organic Framework for the diazinon removal from the real samples

Article *in* Journal of Molecular Structure · May 2021

DOI: 10.1016/j.molstruc.2021.130607

CITATIONS
2

READS
26

4 authors, including:

Vahid Ashouri

8 PUBLICATIONS **51** CITATIONS

SEE PROFILE

Kourosh Adib

Imam Hossein University

34 PUBLICATIONS **324** CITATIONS

SEE PROFILE

Masoumeh Ghalkhani

Shahid Rajaee University

89 PUBLICATIONS **1,472** CITATIONS

SEE PROFILE

Journal of Molecular Structure 1240 (2021) 130607

Contents lists available at ScienceDirect

Journal of Molecular Structure

journal homepage: www.elsevier.com/locate/molstr

Preparation of the extruded UiO-66-based Metal-Organic Framework for the diazinon removal from the real samples

Vahid Ashouri[a], Kourosh Adib[a,*], Mehdi Rahimi Nasrabadi[b,c], Masoumeh Ghalkhani[d]

[a] Department of Chemistry, Faculty of Science, University of Imam Hossein, Tehran, Iran
[b] Chemical Injuries Research Center, Systems Biology and Poisonings Institute, Baqiyatallah University of Medical Sciences, Tehran, Iran
[c] Faculty of Pharmacy, Baqiyatallah University of Medical Sciences, Tehran, Iran
[d] Electrochemical Sensors Research Laboratory, Department of Chemistry, Faculty of Science, Shahid Rajaee Teacher Training University, Tehran, Iran

ARTICLE INFO

Article history:
Received 29 January 2021
Revised 17 April 2021
Accepted 2 May 2021
Available online 10 May 2021

Keywords:
Metal-Organic Framework
AE-MOF Uio-66
Adsorption
Diazinon
Activation
Extrusion

ABSTRACT

An adsorbent was introduced for the diazinon (DIZ) adsorption and removal from real samples. A mixture of the activated metal-organic framework (MOF) and a binder was used as an efficient adsorbent. Tetra(4-Sodium sulfonatophenyl)porphyrin was used as a complexing agent to investigate the spectrum of DIZ in Ultraviolet–visible spectroscopy (UV–Vis). The structural properties of the prepared adsorbent were studied by FT-IR, SEM, XRD, TGA, ^{31}P NMR, and BET methods. To achieve the best efficiency of the DIZ adsorption and removal by the active-shaped Metal-Organic Framework (AE-MOF UiO-66), various practical factors such as pH effect, amount of adsorbent, contact time, and the concentration of the solution specimen were optimized. Under optimized conditions, the linear dynamic range for DIZ determination was 10–500 ng/mL with a limit of detection (LOD) of 2.5 ng/mL. The relative standard deviations (RSD%, $n = 5$) was 3% for the determination of 30.4 ng/mL of DIZ. The study of the adsorption kinetics demonstrated that the rate of DIZ adsorption by AE-MOF UiO-66 correlates well with the pseudo-second-order model. The monolayer adsorption of the DIZ molecules on the AE-MOF UiO-66 surface fits well with the Langmuir isotherm model. A green AE-MOF UiO-66-based adsorbent with a high adsorption capacity was developed for DIZ adsorption and removal from the real specimens.

1. Introduction

Nowadays, pesticides are widely used to eliminate pests from agricultural products. Unfortunately, published reports represent the improper use of pesticides by farmers [1]. Therefore, a massive amount of pesticides are left unused in natural ecosystems. Organophosphorous pesticides (OPPs) are widely utilized as insecticides to enhance farming crops [2]. Also, these pesticides are almost inexpensive and have a significant killing effect on different types of pests [3]. They can be absorbed by aspiration, ingestion, and direct contact with the skin, thus has harmful impacts on marine, earthly species, and humans living around them. OPPs hamper acetylcholinesterase in the nervous system of humans, causing respiratory, myocardial, and neuromuscular disorders [4]. The entry of OPPs residues in agricultural lands into the groundwaters and agricultural products and foodstuffs can create health problems for consumers [5]. Diazinon (DIZ) is an insecticide usually utilized in farming and land management for controlling insects. The World Health Organization (WHO) has declared the critical toxicity level of 300 mg/kg with moderate risk (class 2), and a probable carcinogenic effect for DIZ [6]. The approved pesticides dose in water is about 0.5–0.1 ng/mL [7]. The inhibitory effect of DIZ on the activity of the enzyme acetylcholinesterase causes the abnormal increment of the acetylcholine (a neurotransmitter) within the nervous system resulting in the death of insects. The drastic intestinal torsion, asthma, vision blurriness, migraine, diarrhea, high blood pressure, coma, neuropsychiatric complications such as depression and memory loss, peripheral nervous system diseases, and sensitivity to particular chemical substances are some toxic signs of DIZ [8]. Therefore, exposure to this substance for a long time will be very risky for humans. Hence, efficient decontamination of OPPs, as well as their accurate detection is a critical urgency. Some organophosphates were detected by UV–Vis spectroscopy with the aid of complexing agents. The absorbance shift in the UV–Vis spectrum of the Tetra(4-Sodium sulfonatophenyl)porphyrin-based ligands upon interacting with DIZ was utilized for DIZ detection [9]. Hence, the OPPs determination and reduction of their environmental impacts have become a universal necessity. Various procedures have been considered for impressive removal of OPPs from contaminated samples, including electrochemical degradation [10],

* Corresponding author.
E-mail address: k_anbaz@yahoo.com (K. Adib).

https://doi.org/10.1016/j.molstruc.2021.130607
0022-2860/

adsorption and separation methods [11-14], enzymatic biodegradation [15], and photocatalysis [16]. Between them, the adsorption technique is considered as a competitive method regarding its simple and economical operation. Hence, designing newfound sorbents with substantial adsorption capacity to remove persistent OPPs from the environment is a challenge [17]. DIZ is an OPP that its removal from the natural environment requires sample preparation [18]. Principally, the removal methods of pesticides should not cause environmental pollution; hence green chemistry methods have been noticed. Green chemistry principles are focused on diminishing solvent consumption, employing organic solvent-free methods, miniaturization of strategies, and utilization of the indigenous adsorbents that are renewable and safe biomaterials [19-21].

Over the past decade, metal-organic frameworks (MOFs) have been developed [22-24] as a novel class of eco-friendly solid sorbents [25]. In contrast to prevalent solid adsorbents such as zeolites [26], activated carbon [27], and silica-based materials [28, 29], metal-organic frameworks with versatile framework compositions, tunable pore sizes, attainable active sites, and thermal and chemical resistance [30-33] are a suitable option for removal of toxic, hazardous substances such as OPPs [34].

Due to the powdery state, most MOFs are very soft and sticky, which makes difficult their transfer, separation, and recovery from the contaminated samples, and thus diminishes their adsorption capacity. It is important to overcome these limitations while the adsorption capacity of MOFs retained unchanged. These problems can be eliminated with the appropriate shaping and activation of the adsorbent materials. Adsorbent shaping with proper particle dimension and density is noteworthy [35]. In addition, eliminating guest molecules from the framework while maintaining structural integrity leaves a lot of porosity (i.e., “activation”) [36-38]. Although there are many reports on the effect of forming conditions on adsorbent performance, few studies have been reported focusing on the shape effect on the adsorption capacity. Considering the lack of any report concerning DIZ removal utilizing active-shaped UiO-66-based metal-organic frameworks (AE-MOF UiO-66), high-performance procedure was developed for the DIZ removal from the real specimens.

2. Experimental

2.1. Chemical materials

DIZ was received from the Ministry of Agriculture (the Agricultural Support Services Co., Tehran, Iran). A 300 mg/L DIZ solution was prepared by dissolving a proper amount of DIZ in methanol and doubly distilled water (DDW, 18 MΩ.cm). Dimethylformamide, cyclohexane, porphyrin, terephthalic acid, nitrocellulose, castor oil, zirconium chloride, and all other chemicals were purchased from Merck Co. (Darmstadt, Germany) with analytical grade. The DIZ solutions with given concentrations were prepared simply by diluting its standard solution. The buffer solutions based on NaH_2PO_4 and H_3PO_4 were prepared, and their pH adjustment was carried out using 0.1 M HCl or NaOH solutions.

2.2. Instruments

Ultraviolet-Visible (UV–Vis) spectroscopy tests were done using UV–Vis spectroscopy of Perkin Elmer Company (Lambda 45). Fourier transform infrared (FT-IR) spectra (4000–400) were obtained by an FT-IR spectrometer of Perkin Elmer Company (Spectrum 100). The ^{31}P NMR spectra were recorded at room temperature in D_2O on a Bruker AVANCE 300-MHz instrument (Bruker, Germany). Furthermore, the crystalline structure was determined using XRD analysis (X’PertPRO; PANa-lytical). Specific surface area and pore volume were estimated utilizing the BET (MicroActive for TriStar II plus Version 2.03). A ZEISS Supra 40 SEM with FEG (Field Emission Gun) emitter operating at 10 kV was utilized for the morphology evaluation. Thermogravimetric tests were performed using a thermogravimetry analyzer (TGA, TGD-9800, Advance Riko, Japan). A Metrohm 781 pH, Ion meter (Herisau, Switzerland) equipped with a glass electrode was used to measure the solution’s pH. The two-phase separation was conducted by centrifuging (EBA20, Andreas Hettich GmbH& Co. KG, Zentrifugen, Germany). An AquaMax system (Young- Lin, Korea) was employed to collect deionized water.

2.3. Synthesis and activation of MOF UiO-66

A 40 mL DMF solution containing 0.581 g terephthalic acid and 0.815 g $ZrCl_4$ was transferred into an autoclave lined with Teflon and heated at 120 °C for one day. The resulted product was collected by 10 min centrifuging of the reaction solution at 7000 rpm and then heated at 100 °C for 120 min [39]. The obtained powder was dispersed in methanol and leave it for three days. Then, the process was followed by cyclohexane addition and freezing the reaction mixture at 0 °C, after which the sample was left under ambient conditions. This procedure was subsequently repeated several times, and the sample was finally frozen under vacuum. The soxhlet extraction was carried out for two days to purify the collected white powder, after which it dried at 120 °C for one day. This product was named activated MOF UiO-66.

2.4. Shaping by extrusion

A sample containing nitrocellulose and castor oil mixture in a proportion of 80:20 was prepared. Then, the prepared sample was further mixed with ethyl acetate in a proportion of 15:85, which led to the appearance of an orange color fluid. This composition was employed as a binder to extrude MOF UiO-66. 0.8 g of activated MOF UiO-66 was placed in a 50 mL beaker, and 0.2 g of the prepared binder was added to it. All chemicals were thoroughly mixed and plasticized for 10 min at room temperature. The prepared paste contained 80% (w/v) of the activated UiO-66 MOF and 20% (w/v) of the nitrocellulose-castor oil-ethyl acetate mixture as the binder. The shaping was done by a syringe (nozzle diameter = 0.1 mm). The extruded lines, approximately 100 mm long, were dried for one day at ambient conditions and then were cut into 0.2 mm cylinders (Hereafter referred to as extrude). The final product was named AE-MOF UiO-66.

2.5. Adsorption evaluation

The DIZ adsorption on the AE-MOF UiO-66 was evaluated in the real samples using the batch method. The DIZ complexion with Tetra(4-Sodium sulfonatophenyl)porphyrin has been used to study the UV–Vis spectrum of DIZ. The molecular structure of DIZ and Tetra(4-Sodium sulfonatophenyl)porphyrin was shown in Fig. S1a. This section was performed in a 25 mL beaker under room temperature, which with help of a temperature-controlled water bath, the condition was kept constant. Here, 75 mg of AE-MOF UiO-66 was dispersed in 10 mL DIZ aqueous solution (0.0304 g/L or 0.1 mM). The adsorption variables, including the AE-MOF UiO-66 amount, ionic strength and pH of the solution, contact time, the DIZ concentration, were optimized. Also, the solid phase separation from the solution was very easy. Briefly, 5 min of centrifugation at 3500 rpm was used to ensure complete separation, and at the end, the adsorbent was completely separated from the solution without any observable physical change. (Fig. S1b). In the following, 1 mL Tetra(4-Sodium sulfonatophenyl)porphyrin (2 mM) was

added to the aqueous phase to start the complex formation reaction. Then, the DIZ concentration in maximum absorbance wavelength (λ_{max} = 438 nm) was determined by a UV–Vis spectrophotometer. The DIZ concentration in solution alone or in the presence of adsorbents was measured before and after 15 min stirring (Fig. S2). Three measurements were made for each sample, and the results were averaged. Finally, AE-MOF UiO-66 was studied by infrared spectroscopy and ^{31}P-NMR. The DIZ concentration in the supernatant solution was measured, and the adsorption yield was calculated for each DIZ concentration at equilibrium by using Eq. (1).

$$AE\% = \left[\left(A_i - A_f\right)/A_i\right] \times 100 \quad (1)$$

Where AE% is the adsorption efficiency. A_i and A_f were the primary and final adsorption of DIZ in the solution, respectively. The adsorption capacity was estimated according to the Eq. (2):

$$q_e = (C_0 - C_e)V/m \quad (2)$$

Here, q_e is the adsorption capacity in mg/g. C_0 and C_e are the initial and final concentrations (mg/L) of the analyte, respectively. V and m are the volume of the sample solution (L) and sorbent weight (g), respectively. The sorption capacity (q_e) of AE-MOF UiO-66 for DIZ was obtained equal to 0.38 mmol/g.

2.6. Kinetics of adsorption

The adsorption dose on the surface of a heterogeneous sorbent as a function of time (t) can be estimated by the pseudo-first-order model [40], Eq. (3), and the real interaction between the sorbent and target analyte can be evaluated by the pseudo-second-order model in which the rate-controlling step is related to a chemical adsorption process [41], Eq. (4).

$$Log(q_e - q_t) = Logq_e - (k_1/2.303)t \quad (3)$$

$$t/q_t = 1/k_2 q_e^{\,2} + (1/q_e)t \quad (4)$$

where q_e and q_t are the analyte amount (mg/g) adsorbed on the adsorbent surface at the equilibrium and at any time, t (min), respectively, and k_1 and k_2 are the equilibrium rate constants of the pseudo-first-order adsorption and pseudo-second-order adsorption, respectively.

2.7. Adsorption isotherm

Valuable data about the DIZ adsorption capacity of the AE-MOF UIO-66 was obtained by evaluating the adsorption isotherms. The linear and nonlinear forms of Langmuir, Freundlich, and Redlich-Peterson isotherm models were applied to correlate experimental adsorption data [42, 43]. Monolayer adsorption on a homogeneous surface is described by the Langmuir model, Eqs. (5) and (6), while the Freundlich model characterizes the adsorption reversibility on a heterogeneous surface, Eqs. (7) and (8),

$$C_e/q_e = 1/q_m K_a + C_e/q_m \quad (5)$$

$$q_e = q_m K_a C_e/1 + K_a C_e \quad (6)$$

$$Logq_e = LogK_f + 1/nLogC_e \quad (7)$$

$$q_e = K_f C_e^{\,1/n} \quad (8)$$

The Redlich-Peterson isotherm is a comprehensive equation with K_R, α_R, and g parameters that can be considered as a combination of the Langmuir and the Freundlich isotherms aspects. It illustrates the adsorption equilibrium over a broad range of adsorbate concentrations [44]. The g value varies in the range of 0 to 1. In $g = 1$, the Redlich–Peterson equation turns into the Langmuir equation, while it turns into Henry's law if $g = 0$. This model is formulated as follows:

$$Ln(K_R C_e/q_e - 1) = gLn(C_e) + Ln(a_R) \quad (9)$$

$$q_e = K_R C_e/1 + a_R C_e^{\,g} \quad (10)$$

Moreover, the Temkin isotherm model, Eq. (11), can describe the adsorption capacity by the adsorbent given the hypothesis that the adsorption heat decreases linearly rather than logarithmically [45], as proposed in the Freundlich equation [46].

$$q_e = RT/b_T Ln(A_T C_e) \quad (11)$$

where q_e equal to the value of target compound adsorbed (mg/g) at equilibrium, C_e refers to the analyte concentration in solution (mg/L) at equilibrium, q_m is the maximum adsorption amount (mg/g), k_a is the Langmuir constant revealing the affinity of the binding sites as well as adsorption energy (L/g), k_F is the Freundlich constant (mg/g)(L/mg)$^{1/n}$ relating to the binding capacity, 1/n is Freundlich coefficient or heterogeneity coefficient indicating the deflection from linear adsorption, K_R, α_R, and g ($0 < g < 1$) are isotherm constants, A_T is the equilibrium binding constant representing the maximum value of binding energy (L/g), b_T is the Temkin constant corresponding the adsorption heat (kJ/mol), R is the universal gas constant (8.314 J/mol/K), and T is the absolute temperature (K).

2.8. Real specimens preparation

The water specimens of tap and river were collected from our laboratory (IHU, Tehran, Iran) and Jajrood (Latyan Dam, 10 km northeast of Tehran, Iran), respectively, and filtered using a membrane filter that pore size was 0.45-micron. The tomato and apple samples were obtained from a local shop (Hakimiyeh, Tehran, Iran). After filtration, the collected juice of tomato and apple samples was centrifuged at 4000 rpm for 20 min. To achieve higher recovery and to overcome the high viscosity problems of the collected samples, they were diluted up to 5 fold. Also, in the case of fresh tomato and apple juices, to improve the recovery percentages, the samples were treated by the addition of 500 μL acetone followed by centrifugation at 4000 rpm for 20 min [20, 47]. The filtered supernatant, through a 0.45 μm membrane, was used for DIZ analysis under optimized conditions. Here, 2 mL of prepared real specimens were added to 8 mL of phosphate buffer solution (pH=7, 0.01 M). Then, the pH of the final samples was adjusted with HCl (0.1 M) and NaOH (0.1 M) solutions, then employed for analysis steps.

3. Results and discussion

3.1. Characterization of MOF UiO-66 and DIZ /MOF

Fig. 1 presents the SEM images of the pure and extruded MOF UiO-66. A minor difference appeared between the surface morphology of the untreated and extruded samples. The extrusion process creates some pores in the MOF UiO-66 structures and changes slightly its porous structure, Fig 1b. Meanwhile, the macropore feature of the sample was retained after extrusion.

The crystalline properties and the XRD spectra of MOF UiO-66 and AE-MOF UiO-66 were evaluated by the XRD analysis. XRD patterns of untreated and extruded MOF UiO-66 matched well with the XRD spectra of the simulated sample with the appearance of three distinct peaks in 2θ = 7.5, 8.5, and 26 [48]. As a result, it

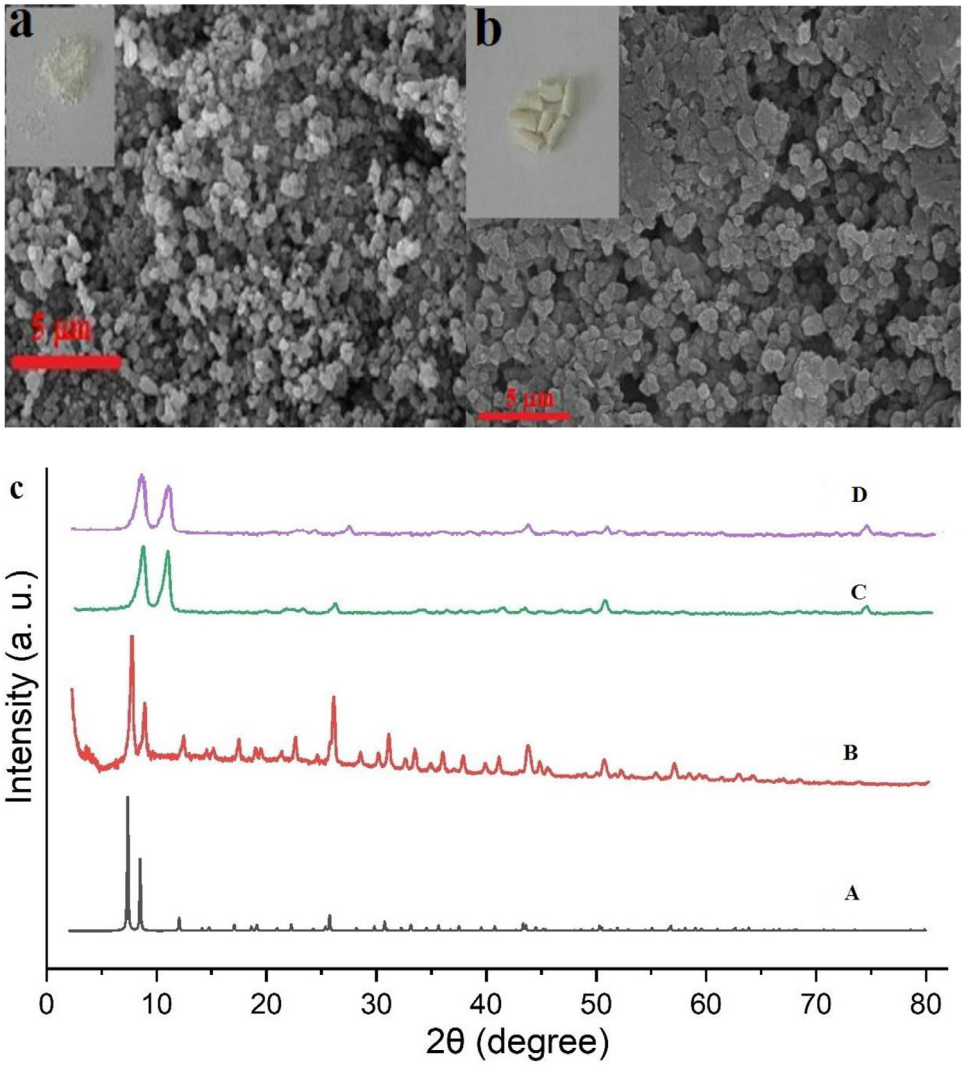

Fig. 1. (a) The SEM images of the MOF UiO-66 (b) AE-MOF UiO-66. (c) X-ray diffraction patterns of the (A) simulated, (B) MOF UiO-66, (C) AE-MOF UiO-66 and (D) AE-MOF UiO-66 of after adsorption.

Table 1
SBET, SBJH, DBJH, and V for MOF UiO-66.

Sample	$S_{BET}(m^2/g)$	$S_{BJH}(m^2/g)$	$D_{BJH}(nm)$	$V(cm^3/g)$ (p/p0=0.99)
MOF UiO-66	1201.3	1136.9	1.95	0.58
AE-MOF UiO-66	710.1	685.2	2.87	0.16

was revealed that the extrusion process didn't change the adsorbent structure crystallographically (Fig. 1c). To confirm the successful adsorption of DIZ on the AE-MOF UiO-66, the ^{31}P NMR spectra of the AE-MOF UiO-66 before and after DIZ (30.4 μg/L) adsorption were recorded (Fig. S3). An intense signal appeared at 30 ppm, originated from DIZ molecules revealing that AE-MOF UiO-66 can effectively adsorb DIZ molecules. Furthermore, the size and volume of the pores in the prepared MOFs, besides their specific surface area, were determined by BET procedure in which the ultrapure nitrogen adsorption of MOFs was evaluated by a Quantachrome NOVA 1000 series analyzer at 77 K. The acquired data were listed in Table 1. The pore diameters of 1.95 nm and 2.87 nm and pore volumes of 0.58 cm^3/g and 0.16 cm^3/g were estimated for MOF UIO-66 and AE-MOF UiO-66 samples, respectively. The high porosity and consequently the high adsorption capacity of prepared MOFs are beneficial for DIZ removal from real samples.

Fig. S4 demonstrates the weight-loss profiles of MOF UIO-66 with two distinguish weight loss regions. The observed weight-loss in the range of 75 °C to 125 °C was related to removing adsorbed water on the MOF UiO-66 surface. The second region weight reduction occurred between 500 °C and 600 °C as the result of MOF UiO-66 decomposition to ZrO_2 [49]. From 600 °C to 800 °C, no clear weight loss was observed in the TG plot, supporting the formation of ZrO_2 that its higher thermal stability is evident. In this study, the temperature used for UiO-66 is much lower than the thermal stability reported up to 480 °C. The observed higher thermal stability of the prepared UIO-66-based MOFs is probable resulted from solvent exchange process, which removed more DMF and nonbonding terephthalic acid from the porous structure of the product.

3.2. Optimization of the procedure conditions

Different factors affecting the developed adsorption procedure, including sample pH, sorbent amount, contact time, salt effect, and

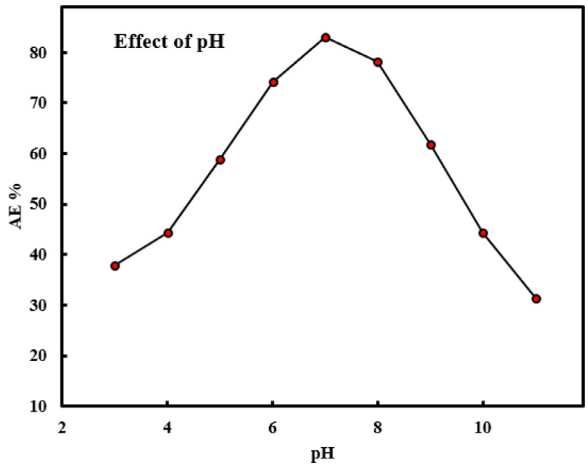

Fig. 2. Assessment of the pH effect on the adsorption and removal of DIZ by the AE-MOF UiO-66. Adsorption conditions: 10 mL sample, 0.0304 g/L DIZ in phosphate buffer (0.01 M); 20 min contact time, 50 mg adsorbent, 2.5% (w/v) salt.

primary sample concentration, were studied. DIZ aqueous solutions with 0.1 M concentration were used for optimization tests.

3.2.1. pH influence

Considering that the pH of the solution is effective in the adsorption performance, the adsorption of 0.1 mM DIZ (0.0304 g/L) from solution with various pH amounts was examined. The buffer solutions prepared by phosphoric acid and its related salts (pH range of 3 to 11) with a total concentration of 0.1 M was employed in this test. DIZ solutions (10 mL) were passed through a column consisting of 0.05 g adsorbent, after which the DIZ concentration was determined after the adsorption process occurred (Fig. 2). An enhancement in DIZ removal was observed by increasing the pH from 3 to 7, while the removal efficiency decreased with further pH increment. As a result, the pH = 7 was selected as an optimum value for further works in the next steps.

3.2.2. Effect of the sorbent dose

The influence of the sorbent dose (10 to 100 mg) on the adsorption efficiency of DIZ from a 10 mL sample solution with 0.1 mM (0.0304 g/L) concentration was evaluated that showed an enhancement in the DIZ adsorption following the increment of the sorbent amount (Fig. S5). The increment of sorbent amount in the mentioned dose range led to providing more accessible sorption sites. The maximum DIZ removal was occurred when 0.075 g sorbent was used. Since no further enhancement in removal was achieved above 0.075 g, this value was selected as the optimum adsorbent dose in further experiments.

3.2.3. DIZ concentration effect

The influence of the primary concentration of DIZ on the adsorption process was studied for concentrations of 0.007–0.042 g/L utilizing a constant weight of AE-MOF UiO-66. A higher percentage of DIZ removal was observed at lower concentrations (Fig. S6). Notably, the decrease in AE%, with the C_0 increment reveals the effect of the mass transfer as a driving force.

3.2.4. Influence of the contact time

Considering that adsorption occurs under the mass transfer phenomenon, the contact time of the analyte solution with sorbent will affect the removal efficiency. The role of contact time on the DIZ removal by AE-MOF UiO-66 was examined, and results were plotted in Fig. S7. The value of DIZ removal by AE-MOF UiO-66 was initially enhanced by increasing time up to 30 min, and after that remained unchanged. The amount of DIZ adsorption at the time of equilibrium indicates the maximum capacity of the sorbent under the operational situation. Fig. S8 demonstrates the incredible impact of the contact time on the DIZ adsorption efficiency. According to the results, the 30 min contact time was chosen for further tests.

Table 2
Isotherm parameters and calculated correlation coefficients.

Model	Parameters	Values
Langmuir	Q_m (mg/g)	4.4
	K_L (L/mg)	0.2
	R^2	0.99
Freundlich	n	1.06
	K_F (mg.g)	0.91
	g	0.95
Redlich–Peterson	α_R	7.22
	R^2	0.65
Temkin	2.45	K_T
	0.45	R^2

3.2.5. Impact of salt

For many organic analytes, it has been observed that the adsorption yield is improved by increasing the ionic strength and consequently lowering their solubility in the aqueous solution (salting-out effect). Meantime, the sample ionic strength has an inverse impact and decreases the adsorption efficiency due to variation of density and solubility parameters. The effect of the NaCl concentration (0 to 10% (w/v) on the DIZ extraction efficiency was evaluated (Fig. S8). The DIZ removal was increased by increasing NaCl concentration up to 2.5% (w/v). Further salt addition decreased the DIZ removal; hence the developed method is applicable for a solution with a maximum 2.5% (w/v) salt content.

3.3. Kinetics of adsorption

The kinetic of DIZ removal from a solution with the primary concentration of 0.1 mM (0.0304 g/L), at pH 7 and ambient temperature using 0.075 mg/mL AE-MOF UiO-66 adsorbent was studied using the pseudo-first-order and pseudo-second-order models. The plots of log (q_e - q_t) as a function of time showed a weak linear relationship with low R^2 (Fig. 3, Table S1). It was revealed that DIZ adsorption on AE-MOF UiO-66 does not obey the pseudo-first-order model. On the other hand, a high correlation was observed between t/q_t and time, confirming that experimental data fit well with the pseudo-second-order model ($R^2 > 0.999$). The q_e, K_2, and the initial adsorption rate [$kq_e^2 = h$ (mg g $^{-1}$min^{-1})] were obtained using the slope and the intercept, respectively, of the plot of t/q_t versus time (Fig. 3 and Table S1). Therefore, the pseudo-second-order model was proposed for the kinetic of the DIZ adsorption by AE-MOF UiO-66.

3.4. Adsorption isotherm

A useful adsorption system can be designed considering the probable interactions between adsorbents and solute based on adsorption isotherms. Hence, finding the suitable isotherm model, which correlates well with the experimental data, is important because it can be used for design purposes. Therefore, four common isotherms, Langmuir, Freundlich, Redlich-Peterson, and Temkin were examined and resulted data were presented in Fig. 4 and Table 2. Here, the best linear correlation was obtained for the plot of (C_e/q_e) versus C_e, revealing that the Langmuir isotherm can explain properly the monolayer adsorption of DIZ on the AE-MOF UiO-66 surface with a limited number of binding sites. Therefore,

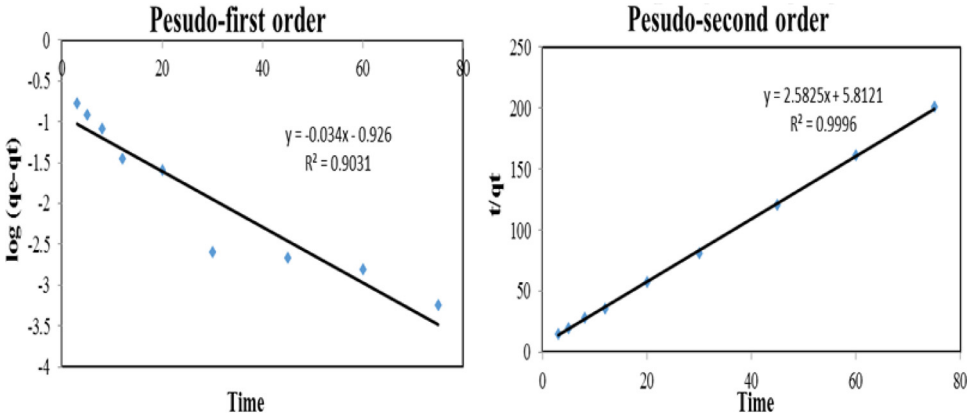

Fig. 3. Pseudo-first order kinetic and Pseudo-second order kinetic for DIZ adsorption on AE-MOF UiO-66 (pH=7).

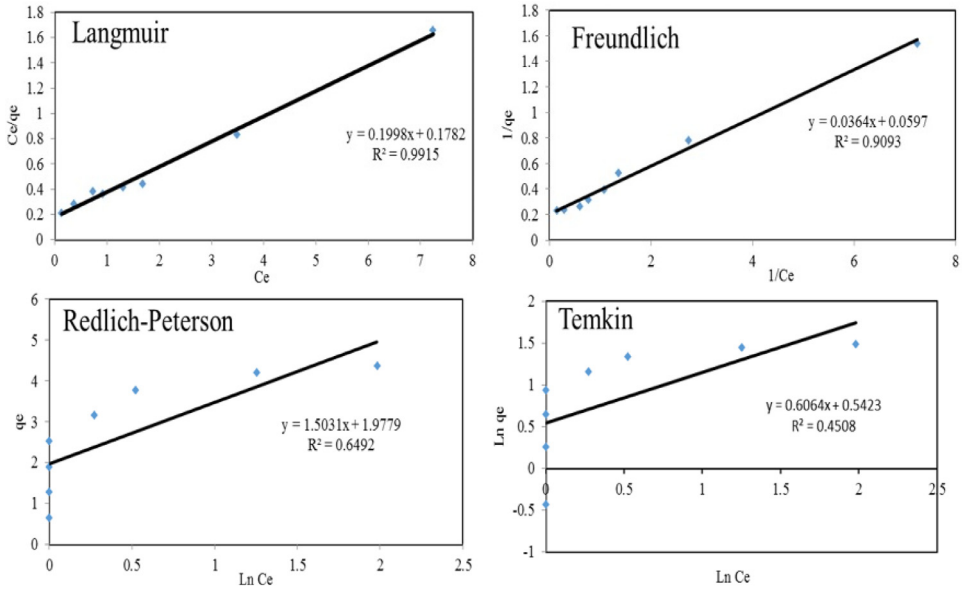

Fig. 4. Linear Langmuir, Freundlich, Redlich-Peterson and Temkin isotherm models for DIZ adsorption using MOF UiO-66 (pH=7).

homogeneous adsorption energies can be assumed without any relocation of DIZ molecules in the framework of AE-MOF UiO-66 surface.

3.5. Mechanism of adsorption

To study the mechanism of the DIZ adsorption process by the AE-MOF UiO-66 adsorbent, FT-IR spectra of DIZ, AE-MOF UiO-66 were acquired before and after the adsorption process. The bands of typical functional groups in the DIZ and AE-MOF UiO-66 structures besides the DIZ adsorbed on the AE-MOF UiO-66 (under optimum conditions) were evaluated in FT-IR spectra to track the probable variations in the FT-IR spectrum after the adsorption process. Details of the distinguished bands in the spectra, with their wavenumbers and band assignments, were as follow:

FT-IR of DIZ (KBr, cm^{-1}): 2977, 1585, 1560, 1471, 1444, 1383, 1349, 1294, 1160, 1099, 1023, 980, 830 and 650. And FT-IR of the AE- MOF UiO-66 (KBr, cm^{-1}): 3435, 2962, 2928, 2854, 1953, 1713, 1661, 1584, 1508, 1395, 1279, 1157, 1105, 1068, 1019, 934, 879, 840, 745, 705, 677, 552, and 476. And FT-IR of DIZ/AE-MOF UiO-66 (KBr, cm^{-1}): 3433, 2975, 2931, 2859, 1953, 1712, 1660, 1587, 1565, 1538, 1507, 1434, 1391, 1354, 1278, 1163, 1102, 1022, 994, 979, 827, 741, 702, 680, 555 and 476 (Fig. 5).

In the FT-IR spectrum of AE-MOF UiO-66 (Fig. 5b), significant peaks originated from the stretching vibration frequencies of the Zr–O_2 and Zr-OH groups were appeared at 702–744 cm^{-1} and 1395 cm^{-1}, respectively. Following the adsorption process (Fig. 5c), a new characteristic peak was observed in the FT-IR spectrum of DIZ/AE-MOF UiO-66 related to the stretching vibration frequencies of P = S in area 979–994 cm^{-1}. Moreover, for the DIZ adsorbed on the AE-MOF UiO-66, the stretching vibration frequencies of C–O, C = N, and C = C could be observed at 1354 cm^{-1}, and the stretching vibration frequencies of 1434 cm^{-1} and 1565 cm^{-1}, respectively. Furthermore, the zeta potential of the AE-MOF UiO-66 was measured to investigate the electrostatic attraction between DIZ and AE-MOF UiO-66. The DIZ has a pK_a = 2.6, which means its molecules have a negative charge at pH=7. According to Fig. 6, the AE-MOF UiO-66 has a negative charge in this pH, which demonstrates negligible electrostatic attraction between AE-MOF UiO-66 and DIZ in pH=7. Notably, the DIZ adsorption onto the AE-MOF UiO-66 might be chemisorption instead of electrostatic adsorption [35]. It is realized that the Zr-based AE-MOF UiO-66 works effectively over a wide range of pH, and its highest removal efficiency for DIZ was observed at pH=7, probably due to the creation of a chemical bond or complex between DIZ and AE-MOF UiO-66. The chemisorption process of DIZ by the AE-MOF UiO-66 may originate from the Zr-OH bonds in MOF, which have a high

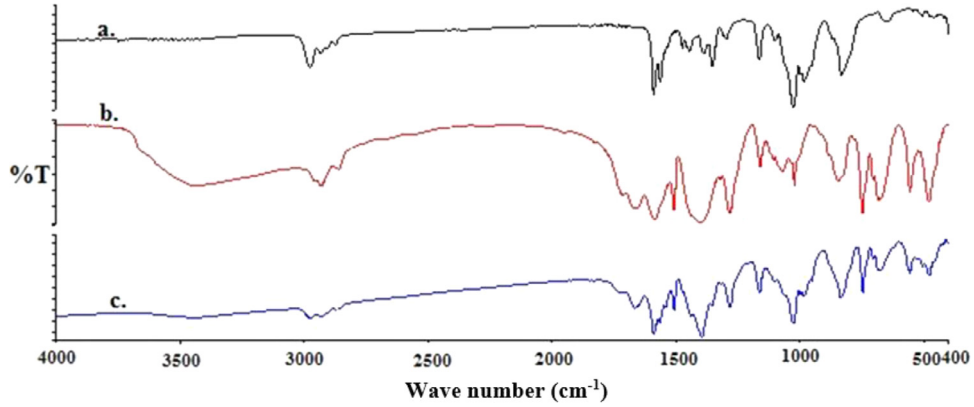

Fig. 5. FT-IR spectra of DIZ (a), MOF UiO-66 (b), and the adsorbed DIZ onto MOF UiO-66 (c), (DIZ solution: 0.0304 g/L, contact time: 20 min, pH = 7).

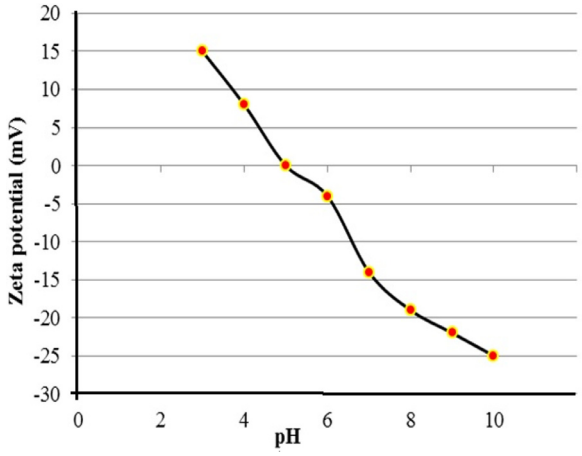

Fig. 6. Zeta potential of AE-MOF UIO-66 in water under different pH values at 25 °C.

Table 3
Analytical characteristics for DIZ analysis.

Analytical parameters	Value
Linear range (ng/mL)	10–500
Coefficient of determination (R^2)	0.999
Slope	1.37
Intercept	0.62
Limit of detection (ng/mL) ($3S_B/m$, $n = 5$)	2.5
Precision (RSD,%) (100 ng/mL, $n = 5$)	3

affinity toward DIZ that is in agreement with the pseudo-second order model.

3.6. Analytical performance

The adsorption efficiency of the AE-MOF UiO-66 and MOF UiO-66 powders for DIZ removal was compared. Here, the DIZ content in the supernatant solution was measured by Ultraviolet–visible spectroscopy (UV–Vis) before and after the adsorption process performed under the optimized conditions. The obtained spectra after the adsorption process presented in Fig. 7 indicate the higher adsorption capacity of the AE-MOF UiO-66 compared to the MOF UiO-66 powder as the adsorption value at $\lambda = 438$ nm is lower in the case of AE-MOF UiO-66. The calibration curve of the established procedure for the determination of DIZ under optimum circumstances represented a linear relation in the range of 10–500 ng/mL with an R^2 value of 0.999 and the detection limit of 2.5 ng/mL (Table 3). The precision of the technique in terms of the relative standard deviation (RSD%), was assessed for 5 replicates determination of 30.4 ng/mL DIZ. The RSD = 3% resulted that verified the acceptable precision of the developed procedure.

Table 4
DIZ determination in real specimens.

Sample	Spiked concentration (mg/L) of DIZ	Recovery (%) ± SD, $n = 3$
Tap water	–	–
	10	94.2 ± 3.8
	20	95.6 ± 2.9
	30	97.8 ± 3.5
River water	–	–
	10	96.1 ± 2.9
	20	97.4 ± 3.8
	30	95.2 ± 3.6
Tomato juice	–	–
	10	85.7 ± 3.1
	20	87.0 ± 3.8
	30	86.0 ± 2.9
Apple juice	–	–
	10	86.2 ± 1.9
	20	86.7 ± 2.6
	30	86.8 ± 2.2
Tomato juice *	–	–
	10	94.9 ± 3.4
	20	96.1 ± 2.0
	30	95.7 ± 2.5
Apple juice *	–	–
	10	95.8 ± 2.8
	20	95.4 ± 2.3
	30	95.9 ± 2.3

The developed adsorption procedure based on AE-MOF UiO-66 was applied for DIZ removal from various real specimens. The real samples were spiked with DIZ at a given concentration, and the DIZ removal and recovery tests were examined, and obtained data were presented in Table 4. Obviously, the matric of real samples had no sensible impact on the DIZ adsorption. Notably, as mentioned in Section 2.8, in the case of apple and tomato juice as real samples, treatment with acetone was performed. Comparing the recovery results of the analyses with or without acetone treatment revealed that for quantitative analysis, this treatment is necessary. In contract, the qualitative analysis can be successfully done on the untreated samples. Moreover, the adsorbent can be easily separated for the sample solution after reaching the adsorption equilibrium; as a result, the UV–Vis analysis step can be done without any problem.

The performance of the AE-MOF UiO-66 toward DIZ removal was compared with previously reported works, Table 5, which indicates comparable sorption capacity (q_e) and wide range of quantification of a small aliquot of sample solution resulted by a minor

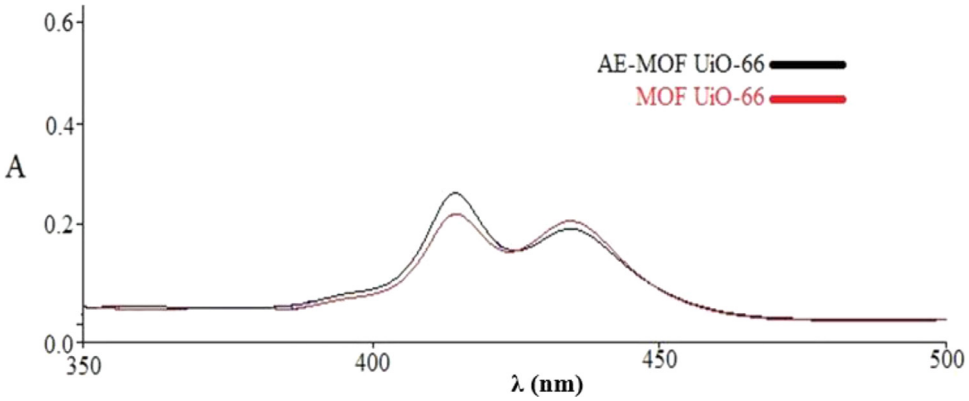

Fig. 7. The UV–Vis spectra recorded after DIZ adsorption process by the AE-MOF UiO-66 and MOF UiO-66 powders.

Table 5
Comparison of analytical characteristics of the developed sorbent with other sorbents for DIZ removal.

Ref	Sample type	Sorption capacity q_e (mg/g)	Sample volume (mL)	Sorbent amount (mg)	Dynamic range	sorbent
[50]	Water	8	25	500	–	MWCNT
[51]	Water	25.6	–	20	–	MCM-41 and MCM-48 mesoporous
[52]	Water	24.69	–	10–100	–	Loess
[53]	Water	58.8	30	50	–	Iron modified
[54]	Water	15–62	100	350	–	ATZ- MZ
This work	Water, Tomato juice and Apple juice	116	10	75	10–500	AE-MOF UiO-66

amount of sorbent [50-54]. It is noteworthy that compared to other mentioned sorbents, the AE-MOF UiO-66 as a green sorbent can be employed for environmental decontamination purposes regarding its benefits such as cheapness, eco-friendly, and easy operation conditions for DIZ removal in a neutral pH.

4. Conclusion

Here, MOF UiO-66 was activated, extruded and utilized as a sorbent for the adsorption and removal of DIZ. The utilized adsorbent illustrates some advantages such as being eco-friendly, recoverable, nontoxic, economical, and having extraordinary adsorbent capacity. The adsorption mechanism of the DIZ by AE-MOF UiO-66 correlated with a pseudo-second-order model based on Langmuir isotherm. The DIZ analysis based on separation and preconcentration with developed sorbent was performed simply for diverse real samples with recovery percentages of 85.7 –97.8%. Also, the DIZ analysis was done in the range of 10–500 ng/mL and a LOD of 2.5 ng/mL resulted. The easy separation of the adsorbent from the sample solution after the adsorption process and facile recovery of the sorbent are other benefits of prepared sorbent. As a powerful sorbent, AE-MOF UiO-66 confirmed a promising role in the pesticides removal and therefore overcoming environmental problems.

Author's statement

Mr. Vahid Ashouri propose the research, synthesis and characterize AE-MOF UiO-66 acquire various adsorption data, Dr. Masoumeh Ghalkhani Conceptualization, Visualization, Writing and editing manuscript, Dr. Kourosh Adib and Prof. Mehdi Rahimi-Nasrabadi provide all facility and investigate the different data and furthermore edited the manuscript.

Declaration of Competing Interest

The authors declare that they have no known competing financial interests or personal relationships that could have appeared to influence the work reported in this paper.

Supplementary materials

Supplementary material associated with this article can be found, in the online version, at doi:10.1016/j.molstruc.2021.130607.

References

[1] J. Kaushal, M. Khatri, S.K. Arya, A treatise on Organophosphate pesticide pollution: current strategies and advancements in their environmental degradation and elimination, Ecotoxicol. Environ. Saf. 207 (2020) 111483.
[2] L.G. Costa, Current issues in organophosphate toxicology, Clin. Chim. Acta 366 (2006) 1–13.
[3] V. Wanjeri, C. Sheppard, A. Prinsloo, J. Ngila, P. Ndungu, Isotherm and kinetic investigations on the adsorption of organophosphorus pesticides on graphene oxide based silica coated magnetic nanoparticles functionalized with 2-phenylethylamine, J. Environ. Chem. Eng. 6 (2018) 1333–1346.
[4] J. Yao, Z. Wang, L. Guo, X. Xu, L. Liu, L. Xu, S. Song, C. Xu, H. Kuang, Advances in immunoassays for organophosphorus and pyrethroid pesticides, TrAC Trends Anal. Chem. (2020) 116022.
[5] N. Sankararamakrishnan, A.K. Sharma, R. Sanghi, Organochlorine and organophosphorous pesticide residues in ground water and surface waters of Kanpur, Uttar Pradesh, India, Environ. Int. 31 (2005) 113–120.
[6] M. Amani, A. Latifi, K. Tahvildari, R. Karimian, Removal of diazinon pesticide from aqueous solutions using MCM-41 type materials: isotherms, kinetics and thermodynamics, Int. J. Environ. Sci. Technol. 15 (2018) 1301–1312.
[7] M.H. Dehghani, Z.S. Niasar, M.R. Mehrnia, M. Shayeghi, M.A. Al-Ghouti, B. Heibati, G. McKay, K. Yetilmezsoy, Optimizing the removal of organophosphorus pesticide malathion from water using multi-walled carbon nanotubes, Chem. Eng. J. 310 (2017) 22–32.
[8] B. Maddah, S.S. Javadi, A. Mirzaei, M. Rahimi-Nasrabadi, Application of electrospun polystyrene nanofibers as solid phase extraction sorbent for the preconcentration of diazinon and fenitrothion in environmental waters, J. Liq. Chromatogr. Relat. Technol. 38 (2015) 208–214.
[9] H. Cao, J. Nam, H.J. Harmon, D.H. Branson, Spectrophotometric detection of organophosphate diazinon by porphyrin solution and porphyrin-dyed cotton fabric, Dyes Pigm. 74 (2007) 176–180.

[10] Y. Samet, L. Agengui, R. Abdelhédi, Electrochemical degradation of chlorpyrifos pesticide in aqueous solutions by anodic oxidation at boron-doped diamond electrodes, Chem. Eng. J. 161 (2010) 167–172.
[11] B.J. Johnson, A.P. Malanoski, I.A. Leska, B.J. Melde, J.R. Taft, M.A. Dinderman, J.R. Deschamps, Adsorption of organophosphates from solution by porous organosilicates: capillary phase-separation, Microporous Mesoporous Mater. 195 (2014) 154–160.
[12] H.H. Han, Ah.R. Kim, T.H. Kim, Y.S. Bae, Facile Cu(I) loading for adsorptive C_3H_6/C_3H_8 separation through double Cu(II) salts incorporation within pores with unsaturated Fe(II) sites, Bull. Korean Chem. Soc. 42 (3) (2021) 471–476.
[13] S.K. Lee, Y.J. Lee, K. Cho, U.H. Lee, J.S. Chang, A fluorinated metal-organic framework, FMOF-2, for preferential adsorption of ethane over ethylene, Bull. Korean Chem. Soc. 42 (2) (2021) 286–289.
[14] J.I. Choi, D. Moon, H. Chun, Static and dynamic adsorptions of water vapor by cyclic [Zr36] clusters: implications for atmospheric water capture using molecular solids, Bull. Korean Chem. Soc. 42 (2) (2021) 294–302.
[15] S. Anwar, F. Liaquat, Q.M. Khan, Z.M. Khalid, S. Iqbal, Biodegradation of chlorpyrifos and its hydrolysis product 3, 5, 6-trichloro-2-pyridinol by Bacillus pumilus strain C2A1, J. Hazard. Mater. 168 (2009) 400–405.
[16] H. Hossaini, G. Moussavi, M. Farrokhi, The investigation of the LED-activated FeFNS-TiO_2 nanocatalyst for photocatalytic degradation and mineralization of organophosphate pesticides in water, Water Res. 59 (2014) 130–144.
[17] Z. kbarlou, V. Alipour, M. Heidari, K. Dindarloo, Adsorption of diazinon from aqueous solutions onto an activated carbon sample produced in Iran, Environ. Health Eng. Manag. J. 4 (2) (2017) 93–99.
[18] G. Moussavi, H. Hosseini, A. Alahabadi, The investigation of diazinon pesticide removal from contaminated water by adsorption onto NH4Cl-induced activated carbon, Chem. Eng. J. 214 (2013) 172–179.
[19] S. Sadeghi, V. Ashoori, Sequential determination of iron species in food samples by new task specific ionic liquid based in situ dispersive liquid–liquid microextraction prior to flame atomic absorption spectrometry, Anal. Methods 8 (2016) 5031–5038.
[20] S. Sadeghi, V. Ashoori, Iron species determination by task-specific ionic liquid-based in situ solvent formation dispersive liquid–liquid microextraction combined with flame atomic absorption spectrometry, J. Sci. Food Agric. 97 (2017) 4635–4642.
[21] V. Ashouri, K. Adib, M. Rahimi-Nasrabadi, Pre-concentration and extraction of fenitrothion using a prefabricated 3D spongin-based skeleton of marine demosponge: optimization by experimental design, Appl. Phys. A 126 (2020) 1–12.
[22] E. Naghian, E.M. Khosrowshahi, E. Sohouli, F. Ahmadi, M. Rahimi-Nasrabadi, V. Safarifard, A new electrochemical sensor for the detection of fentanyl lethal drug by a screen-printed carbon electrode modified with the open-ended channels of Zn (ii)-MOF, New J. Chem. 44 (22) (2020) 9271–9277.
[23] E. Naghian, F. Shahdost-fard, E. Sohouli, V. Safarifard, M. Najafi, M. Rahimi–Nasrabadi, A. Sobhani-Nasab, Electrochemical determination of levodopa on a reduced graphene oxide paste electrode modified with a metal-organic framework, Microchem. J. 156 (2020) 104888.
[24] E. Sohouli, M.S. Karimi, E.M. Khosrowshahi, M. Rahimi-Nasrabadi, F. Ahmadi, Fabrication of an electrochemical mesalazine sensor based on ZIF-67, Measurement 165 (2020) 108140.
[25] W.Y. Hong, S.P. Perera, A.D. Burrows, Manufacturing of metal-organic framework monoliths and their application in CO_2 adsorption, Microporous Mesoporous Mater. 214 (2015) 149–155.
[26] I. Javed, F. Mateen, U. Rafique, N. Tabassum, K.S. Balkhair, M. Aqeel Ashraf, Synthesis of zeolite from marble powder waste: a greener approach and its application for the removal of inorganic metals from wastewater, Desalin. Water Treat. 57 (2016) 10422–10431.
[27] A. Ahmadpour, N. Eftekhari, A. Ayati, Performance of MWCNTs and a low–cost adsorbent for Chromium (VI) ion removal, J. Nanostruct. Chem. 4 (2014) 171–178.
[28] H.J. Kim, H.C. Yang, D.Y. Chung, I.H. Yang, Y.J. Choi, J.k Moon, Functionalized mesoporous silica membranes for CO_2 separation applications, J. Chem. 1-9 (2015) 202867 ID.
[29] X. Liu, A. Wang, L. Li, T. Zhang, C. Mou, J. Lee, synthesis of Au-Ag Alloy nanoparticles supported on silica gel via galvanic replacement reaction, Progress Nat. Sci.: Mater. Int. 23 (2013) 317–325.
[30] N.S. Bobbitt, M.L. Mendonca, A.J. Howarth, T. Islamoglu, J.T. Hupp, O.K. Farha, R.Q. Snurr, metal-organic frameworks for the removal of toxic industrial chemicals and chemical warfare agents, Chem. Soc. Rev. 46 (2017) 3357–3385.
[31] A. Cadiau, K. Adil, P. Bhatt, Y. Belmabkhout, M. Eddaoudi, A metal-organic framework–based splitter for separating propylene from propane, Science 353 (2016) 137–140.
[32] S. Jang, S. Jee, R. Kim, J.H. Lee, H.Y. Yoo, W. Park, J. Shin, K.M. Choi, Heterojunction of pores in granola-type crystals of two different metal-organic frameworks for enhanced formaldehyde removal, Bull. Korean Chem. Soc. 42 (2) (2021) 315–321.
[33] D. Song, J. Bae, H. Ji, M.B. Kim, Y.S. Bae, K.S. Park, D. Moon, N.C. Jeong, Coordinative reduction of metal nodes enhances the hydrolytic stability of a paddlewheel metal-organic framework, J. Am. Chem. Soc. 141 (19) (2019) 7853–7864.
[34] Z. Ni, J.P. Jerrell, K.R. Cadwallader, R.I. Masel, Metal-organic frameworks as adsorbents for trapping and preconcentration of organic phosphonates, Anal. Chem. 79 (2007) 1290–1293.
[35] Y. Khabzina, J. Dhainaut, M. Ahlhelm, H.-J. Richter, H. Reinsch, N. Stock, D. Farrusseng, Synthesis and shaping scale-up study of functionalized UiO-66 MOF for ammonia air purification filters, Ind. Eng. Chem. Res. 57 (2018) 8200–8208.
[36] J.E. Mondloch, O. Karagiaridi, O.K. Farha, J.T. Hupp, Activation of metal–organic framework materials, CrystEngComm 15 (2013) 9258–9264.
[37] J. Bae, E.J. Lee, N.C. Jeong, Metal coordination and metal activation abilities of commonly unreactive chloromethanes toward metal–organic frameworks, Chem. Commun. 54 (2018) 6458–6471.
[38] J. Bae, J.S. Choi, S. Hwang, W.S. Yun, D. Song, J.D. Lee, N.C. Jeong, Multiple coordination exchanges for room-temperature activation of open-metal sites in metal-organic frameworks, ACS Appl. Mater. Interfaces 9 (29) (2017) 24743–24752.
[39] I.D. Rahmawati, R. Ediati, D. Prasetyoko, Synthesis of UiO-66 using solvothermal method at high temperature, IPTEK J. Proceed. Series 1 (2014).
[40] J.-P. Simonin, On the comparison of pseudo-first order and pseudo-second order rate laws in the modeling of adsorption kinetics, Chem. Eng. J. 300 (2016) 254–263.
[41] Y. Liu, New insights into pseudo-second-order kinetic equation for adsorption, Colloids Surf. A 320 (2008) 275–278.
[42] K.Y. Foo, B.H. Hameed, Insights into the modeling of adsorption isotherm systems, Chem. Eng. J. 156 (2010) 2–10.
[43] L. Zhang, S. Hong, J. He, F. Gan, Y.S. Ho, Isotherm study of phosphorus uptake from aqueous solution using aluminum oxide, Clean Soil Air Water 38 (2010) 831–836.
[44] P. Gogoi, D. Dutta, T.K. Maji, Equilibrium and kinetics study on removal of arsenate ions from aqueous solution by CTAB/TiO_2 and starch/CTAB/TiO_2 nanoparticles: a comparative study, J. Water Health 15 (2017) 58–71.
[45] C. Aharoni, M. Ungarish, Kinetics of activated chemisorption. Part 2.-Theoretical models, J. Chem. Soc. Faraday Trans. 1 F 73 (1977) 456–464.
[46] Y. Ho, J. Porter, G. McKay, Equilibrium isotherm studies for the sorption of divalent metal ions onto peat: copper, nickel and lead single component systems, Water Air Soil Pollut. 141 (2002) 1–33.
[47] V. Ashouri, M. Rahimi-Nasrabadi, G. Attaran Fariman, K. Adib, M.M. Zahedi, M.R. Ganjali, E. Marzi Khosrowshahi, Extraction and pre-concentration of ketamine by using a three-dimensional spongin-based scaffold of the Haliclona sp. marine demosponge origin, Appl. Phys. A 126 (2020) 1–12.
[48] M.J. Katz, Z.J. Brown, Y.J. Colón, P.W. Siu, K.A. Scheidt, R.Q. Snurr, O.K. Farha, A facile synthesis of UiO-66, UiO-67 and their derivatives, Chem. Commun. 49 (82) (2013) 9449–9451.
[49] H.R. Abid, G.H. Pham, H.-M. Ang, M.O. Tade, S. Wang, Adsorption of CH_4 and CO_2 on Zr-metal organic frameworks, J. Colloid Interface Sci. 366 (2012) 120–124.
[50] T.T. Firozjaee, N. Mehrdadi, M. Baghdadi, G.N. Bidhendi, The removal of diazinon from aqueous solution by chitosan/carbon nanotube adsorbent, Desalin. Water Treat. 79 (2017) 291–300.
[51] M. Armaghan, M.M. Amini, Adsorption of diazinon and fenitothion on MCM-41 and MCM-48 mesoporous silicas from non-polar solvent, Colloid. J. 71 (2009) 583.
[52] F. Pishgar, H.A. Panahi, A.A. Khodaparast Haghi, V. Motaghitalab, A.H. Hasani, Comparative study on adsorptive characteristics of diazinon in water by various adsorbents, J. Chem. 8329650 (2016) 1–7.
[53] P. Kabwadza-Corner, N. Matsue, E. Johan, T. Henmi, Mechanism of diazinon adsorption on iron modified montmorillonite, Am. J. Anal. Chem. 5 (2014) 70–76.
[54] H. Esfandian, A. Samadi-Maybodi, M. Parvini, B. Khoshandam, Development of a novel method for the removal of diazinon pesticide 3 from aqueous solution and modeling by artificial neural networks 4 (ANN), J. Ind. Eng. Chem. 35 (2016) 295–308.